ELSEVIER

Catalysis Today 66 (2001) 475–485

CATALYSIS TODAY

www.elsevier.com/locate/cattod

External and internal mass transfer effect on photocatalytic degradation

Dingwang Chen, Fengmei Li, Ajay K. Ray*

Department of Chemical and Environmental Engineering, The National University of Singapore, 10 Kent Ridge Crescent, Singapore 119260, Singapore

Abstract

A rational approach is proposed in determining the effect of internal and external mass transfer, and catalyst layer thickness during photocatalytic degradation. The reaction occurs at the liquid–catalyst interface and therefore, when the catalyst is immobilized, both external and internal mass transfer plays significant roles in overall photocatalytic processes. Several model parameters, namely, external mass transfer coefficient, dynamic adsorption equilibrium constant, adsorption rate constant, internal mass transfer coefficient, and effective diffusivity were determined either experimentally or by fitting realistic models to experimental results using benzoic acid as a model component. The effect of the internal mass transfer on the photocatalytic degradation rate over different catalyst layer thickness under two different illuminating configurations was analyzed theoretically and later experimentally verified. It was observed that an optimal catalyst layer thickness exists for SC (substrate-to-catalyst) illumination.

Keywords: Photocatalysis; Mass transfer; Catalyst layer thickness; TiO_2; Water purification; Kinetic study

1. Introduction

Semiconductor photocatalytic processes have been studied for nearly 20 years due to their intriguing advantages in environmental remediation. Among the semiconductor photocatalysts tested, Degussa P25 TiO_2 has been proven to be the most active catalyst. TiO_2 catalyst has been used in two forms: suspended in aqueous solutions in the form of slurry, and immobilized onto rigid inert supports. In the former case, a high ratio of illuminated surface of catalyst to the effective reactor volume can be achieved for small well-designed photocatalytic reactor [1] and almost no mass transfer limitation exists since the maximum diffusional distance is very small resulting from the use of ultra-fine (<30 nm) catalyst particles [2]. However, in large-scale applications, the catalyst particles must be filtered prior to the discharge of the treated water, even though TiO_2 is harmless to environment. Besides, the penetration depth of UV light is limited due to the strong absorption by TiO_2 and dissolved organic species. All these disadvantages render the scale-up of a slurry photocatalytic reactor difficult [3,4].

Above problems can be eliminated by immobilizing TiO_2 catalyst over suitable supports [5]. Design and development of immobilized thin catalyst film makes it possible for commercial-scale applications of TiO_2 based photocatalytic processes for water treatment [6,7]. The designs are more likely to be useful in commercial applications as it provides at least three important advantages. Firstly, it eliminates the need for separation of catalyst particles from treated liquid and enables the contaminated water to be treated continuously. Secondly, the catalyst film is porous,

* Corresponding author. Tel.: +65-874-8049; fax: +65-779-1936.
E-mail address: cheakr@nus.edu.sg (A.K. Ray).

0920-5861/01/$ – see front matter
PII: S0920-5861(01)00256-5

Nomenclature

A	surface area of catalyst layer (m^2)
C	concentration (mol/m^3)
D_e	effective diffusivity (m^2/s)
H	catalyst layer thickness (m)
I	light intensity (W/m^2)
k	rate constant, mass transfer coefficient (m/s)
k_a	adsorption equilibrium constant (m^3/mol)
k_f	internal mass transfer resistance factor (m/s)
K	adsorption rate constant (s^{-1})
m	catalyst mass (kg)
q	adsorption capacity (mol/kg)
r	reaction rate (mol/s m^2)
R	radius of illuminated window (m)
S	surface area of catalyst particle (m^2)
t	time (s)
v	liquid volume (m^3)
z	axial position (m)

Greek letters

α	light adsorption coefficient (m^{-1})
ε	porosity of the catalyst layer
λ	light wavelength (nm)
ρ	density of catalyst particle (kg/m^3)
ϕ	Thiele modulus

Subscript and superscripts

a	exponent of light intensity
b	bulk
d	degradation
e	equilibrium
ext	external
h	photogenerated hole
int	internal
i	light intensity
m	mass transfer
max	maximum
obs	observed
opt	optimal
p	pore, particle
rxn	reaction
s	layer surface, saturated
t	total
0	initial

therefore, it can provide a large surface area for the degradation of contaminant molecules. Thirdly, when a conductive material is used as support, the catalyst film can be connected to an external potential to reduce electron–hole recombination by removing excited electrons, thereby significantly improving the efficiency [8]. However, Immobilization of TiO_2 on supports also creates its own problem [9]. There are at least two obvious problems arising from this arrangement: the accessibility of the catalytic surface to the photons and the reactants, and significant influence of external mass transfer, particularly at low fluid flow rate, due to the increasing diffusional length of reactant from bulk solution to the catalyst surface. While on the other hand, with the increase of catalyst film thickness, the internal mass transfer may play a dominant role by limiting utilization of the catalyst near the support–catalyst interface. All these lead to a lower overall degradation rate when catalyst is immobilized compared with the suspended system [10]. Surprisingly, there are very few investigations, which offer a rational approach to study the influence of mass transfer in immobilized catalyst films. Majority of the researchers has focused on the investigation to the effect of operational parameters on the degradation rate, and on the reactor design aspects. No work on dynamic mass transfer parameters has been reported in literature to the best of our knowledge.

2. Experimental details

The semi-batch photocatalytic reactor used in this study is shown in Fig. 1. Two reactors of same configuration but different dimensions were used in this study. Dynamic physical adsorption experiments were conducted in reactor 1 ($V = 1.88 \times 10^{-5}\,m^3$, $d = 0.073\,m$), which was connected to a Perkin Elmer UV spectrophotometer for on-line measurement of benzoic acid. The second reactor, reactor 2 ($V = 3.8 \times 10^{-5}\,m^3$, $d = 0.05\,m$), was used for the photocatalytic reaction experiments. The lamp (Philips HPR 125 W high-pressure mercury vapour) used has a sharp (primary) peak at $\lambda = 365\,nm$ of 2.1 W, and thereby the incident light intensity was $213\,W/m^2$. A Shimadzu 5000A TOC analyzer with an ASI-5000 autosampler was used to analyze the TOC in samples. Concentration of benzoic acid in the

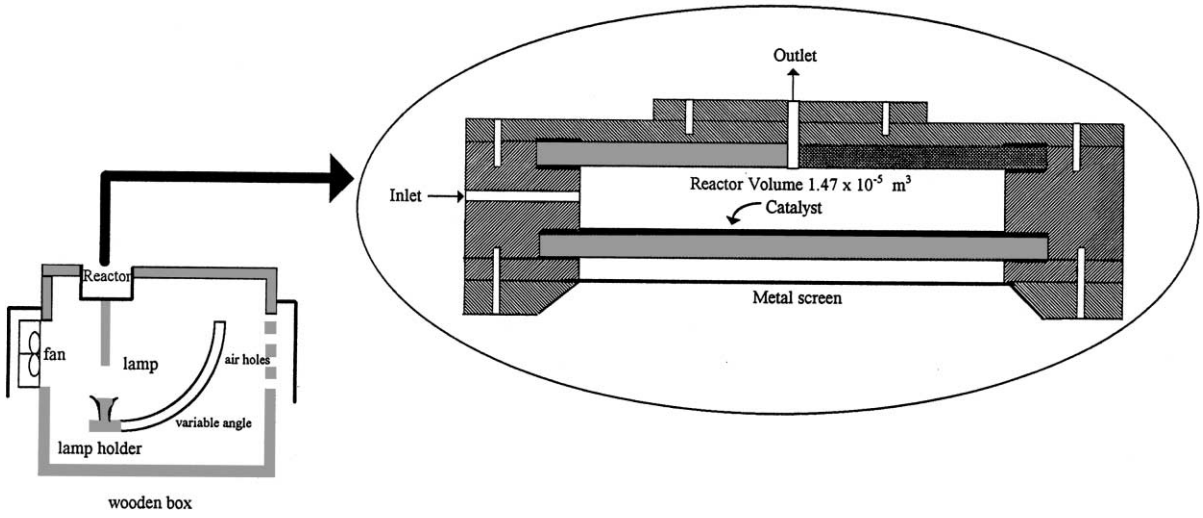

Fig. 1. Schematic diagram of the kinetic reactor.

reaction samples was analyzed by a HPLC (Perkin Elmer LC240). Aliquots of 20 μl were injected onto a reverse-phase C-18 column (Chrompack), and eluted with the mixture of acetonitrile (60%) and ultrapure water (40%) at a total flow rate of 1.5 ml/min. Absorbance at 229 nm was used to measure the concentration of above compounds by a UV/VIS detector (Perkin Elmer 785A). All water samples were filtered by Millex–HA filter (Millipore, 0.45 μm) before analyses. The light intensity was measured by a digital radiometer (UVP model number UVX-36).

In this study, circular Pyrex glass (thickness 0.0032 m) was used as catalyst support. Varied thickness of catalyst film was obtained by controlling the speed of coating and number of times coated using an automated dip-coating apparatus [6]. Subsequently, the coated glass plate was calcined in a furnace. The influence of calcination temperature on reactivity of immobilized catalyst layer was reported in one of our earlier paper [11]. The optimal calcination temperature found out was around 573 K. The total mass of catalyst deposited per unit area was determined by weighing the glass plate before and after the catalyst coating. Subsequently, catalyst layer thickness was calculated based on the density of the catalyst particles and layer porosity. Surface texture measurement of the coated catalyst layer by Taylor–Hobson indicated that catalyst particles were uniformly distributed on the entire glass plate. Scanning electron micrograph pictures illustrating the surface morphology of a roughened (sand blasted) glass plate with no catalyst, and TiO_2 films containing 5.0×10^{-4} kg/m^2 (thin film) and 3.0×10^{-3} kg/m^2 (thick film) has been published elsewhere [1]. The coated catalyst was observed to be stable for a wide range of pH. The TiO_2 immobilized in this way was found to be photocatalytically active, capable of decomposing a variety of organic substances including phenol, 4-chlorophenol, 4-nitrophenol and benzoic acid [2,11].

3. Results and discussions

Experiments were performed to study the photocatalytic degradation rate when catalyst was immobilized either on the bottom plate or on the top plate. In the latter case, light intensity on the catalyst surface is considerably reduced, as it travels through the absorbing liquid medium. The two circumstances can be depicted as SC (substrate–catalyst) and LC (liquid–catalyst) illumination [1]. Fig. 2(a) and (b) represent the cases in which the catalyst-coated glass plate is placed at the top (LC illumination) or at the bottom (SC illumination) respectively for the photocatalytic reactor used in this work.

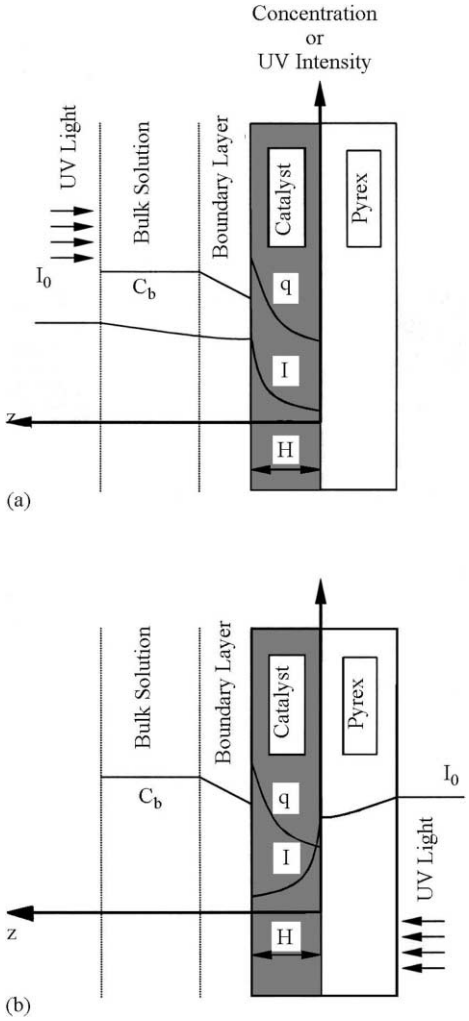

Fig. 2. Schematic diagram of the profiles of concentration and UV light intensity in TiO_2 immobilized system. (a) LC illumination and (b) SC illumination.

In the photocatalytic reaction over immobilized catalyst, both internal and external mass transfer must be considered. The relationship among the observed degradation rate, the external and internal mass transfer rates and the intrinsic kinetic reaction rate are given by the following expression:

$$\left[\frac{1}{k_{\text{obs}}}\right] = \left[\frac{1}{k_{\text{rxn}}}\right] + \left[\frac{1}{k_{\text{m,int}}}\right] + \left[\frac{1}{k_{\text{m,ext}}}\right] \quad (1)$$

In determining the intrinsic kinetic parameters, it is essential to estimate the external mass transfer resistance. At steady state, the mass transfer rate to the catalyst surface, $r_{\text{m,ext}}$, must be equal to the surface catalyzed reaction rate, r_{rxn}: $k_{\text{m,ext}}(C_b - C_s) = k_{\text{rxn}} f(C_s)$, where $f(C_s)$ represents the concentration dependence of the surface catalyzed reaction rate. The external mass transfer coefficient was determined experimentally by measuring the dissolution rate of benzoic acid into water flowing at different flow rates. The result is shown as a function of Reynolds number in Fig. 3 together with the best least square fit, which is correlated by $k_{\text{m,ext}}(\text{in m/s}) = 3.49 \times 10^{-7} Re^{0.77}$.

The internal mass transfer resistance results from the diffusion of organic molecules within the porous catalyst thin film. Influence of the internal mass transfer can be stipulated by the magnitude of Thiele modulus. Assuming the thin catalyst film as a porous slab, the Thiele modulus is defined as: $\phi_H = H[k_v/D_e]^{1/2}$, for the first order reaction. k_v can be determined experimentally by kinetic study at high circulating flow rate over a monolayer of catalyst film. Evidently, effective diffusivity dominates the internal mass transfer process. However, no literature value of effective diffusivity has been reported for organic compounds in porous TiO_2 film. Hence, in this study, the effective diffusivity was determined experimentally. In order to obtain the effective diffusivity, adsorption rate constant, K, need to be first determined by performing the dynamic physical adsorption experiments. The thinnest catalyst film (about 0.63 μm) was used so that the internal mass transfer resistance can be assumed to be negligible. The physical adsorption (dark reaction) process of benzoic acid over a thin TiO_2 catalyst film can be described by the following equations:

$$v\left[\frac{dC_b}{dt}\right] = -k_{\text{m,ext}} A(C_b - C_s), \quad \text{at } t = 0,\ C_b = C_0 \quad (2)$$

$$\frac{dq}{dt} = K\left[\frac{k_a q_s C_s}{(1 + k_a C_s)} - q\right], \quad \text{at } t = 0,\ q = 0 \quad (3)$$

$$v(C_0 - C_b) = mq \quad (4)$$

Rearranging Eqs. (2)–(4) with the assumption that $k_a C_s \ll 1$ at low pollutant concentration, the variation of the bulk concentration of benzoic acid with the adsorption time is

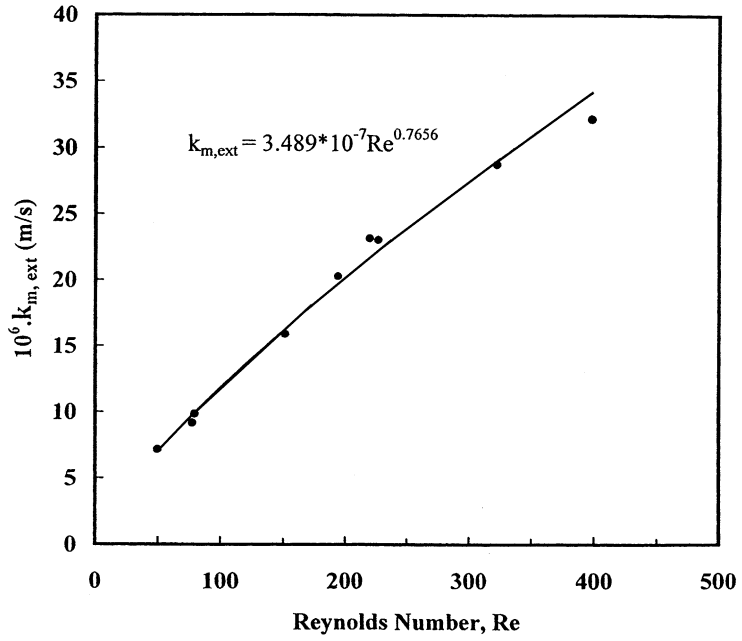

Fig. 3. Measurement of external mass transfer coefficient, $k_{m,ext}$, against Reynolds number.

$$\left[\frac{1}{k_{m,ext}A} + \frac{1}{k_a K m q_s}\right]\frac{dC_b}{dt} = -\left[\frac{1}{v} + \frac{1}{k_a m q_s}\right]C_b + \frac{1}{k_a m q_s}C_0 \quad (5)$$

The analytical solution to Eq. (5) is given by

$$\frac{C_b - C_e}{C_0 - C_e} = \exp\left[-\frac{k_{m,ext}AK(v + mk_a q_s)}{v(k_{m,ext}A + mk_a q_s K)}t\right] \quad (6)$$

In order to obtain a reliable value of K, dynamic physical adsorption experiments were performed. Fig. 4 shows the experimental results alongside the effect of fitted adsorption rate constant values. The optimum adsorption rate constant, K, obtained by best fitting the experimental results to Eq. (6) is $0.2\,s^{-1}$.

Dynamic physical adsorption experiments over a thicker (about 5.3 μm) catalyst layer were performed for three different initial concentrations of benzoic acid in order to determine the effective diffusivity. The process can be described by the following equations:

$$\varepsilon\left[\frac{\partial C_p}{\partial t}\right] = D_e\left[\frac{\partial^2 C_p}{\partial z^2}\right] - \rho_p(1-\varepsilon)\left[\frac{\partial q}{\partial t}\right] \quad (7)$$

$$v(C_0 - C_b) = \left(\frac{m}{H}\right)\int_0^H q\,dz \quad (8)$$

$$\left[\frac{\partial q}{\partial t}\right] = K[q_s - q] \quad (9)$$

$$\text{BC}: \quad k_{m,ext}[C_b - C_p] = D_e\left[\frac{\partial C_p}{\partial z}\right] \quad \text{at } z = 0 \text{ and } t > 0 \quad (10)$$

$$\left[\frac{\partial C_p}{\partial z}\right] = 0 \quad \text{at } z = H \text{ and } t > 0 \quad (11)$$

$$\text{IC}: \quad q = 0,\ C_p = 0,\ C_b = 0 \quad \text{at } t = 0 \quad (12)$$

Porosity of the catalyst layer was taken as 0.34 [8]. Above partial differential equations were solved numerically using control volume based finite difference method. The effective diffusivity of benzoic acid was determined by fitting the experimental data to the solution of the above model. The result is shown in Fig. 5 and a good agreement was obtained when D_e was assumed in the model as $1.0 \times 10^{-10}\,m^2/s$.

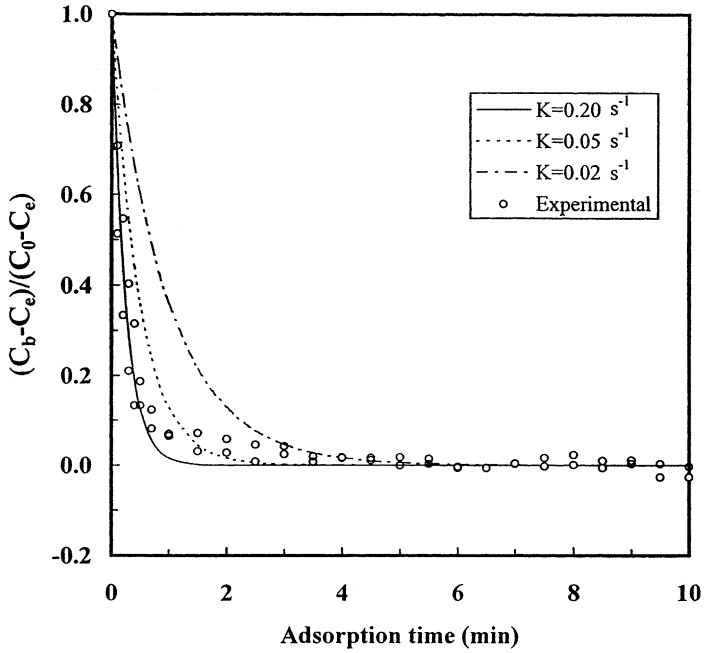

Fig. 4. Determination of adsorption rate constant, K ($m = 6.6\times10^{-6}$ kg, $v = 3.4\times10^{-5}$ m^3, $Re = 141$, $T = 300$ K and $A = 4.17\times10^{-3}$ m^2).

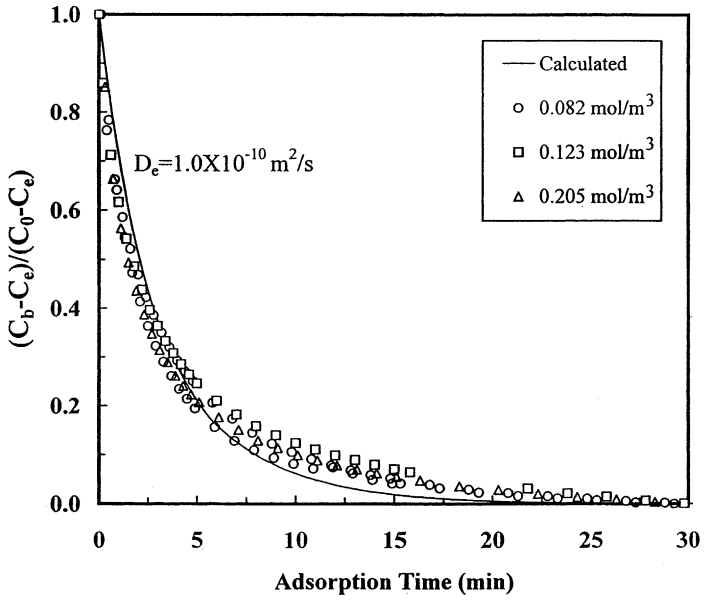

Fig. 5. Determination of effective diffusivity of benzoic acid in TiO_2 catalyst film ($v = 3.2\times10^{-5}$ m^3, $m = 5.51\times10^{-5}$ kg, $K = 0.2$ s^{-1}, $\varepsilon = 0.34$, $\rho_p = 3800$ kg/m^3, $H = 5.27\times10^{-6}$ m, $Re = 141$ and $T = 300$ K).

4. Photocatalytic degradation

It has been well established that when TiO_2 is illuminated by the light of wavelength less than 380 nm in the presence of water containing dissolved organic compounds and oxygen, photocatalytic reactions take place. The concentration of hole (h^+) in the illuminated TiO_2 particles depends on the intensity of the incident light and can be described as $C_h = k_i I^a$, in which the value of a is usually between 0.5 and 1.0 [2]. Thus, the degradation rate of a dissolved organic species on a single illuminated TiO_2 particle is given by $r_p = k_d,\ S_p,\ C_s,\ C_h$. If v_p is the volume of a single catalyst particle, then the number of particles in unit volume of catalyst layer is $(1-\varepsilon)/v_p$, and consequently, the total degradation rate, r_t, for a catalyst layer can be determined by integrating above over the catalyst volume, AH, and is given by

$$r_t = v\frac{dC_b}{dt} = k_i k_d S_p \frac{1-\varepsilon}{v_p}\int_0^H\int_0^R r\int_0^{2\pi} \times C_s I^a \, d\theta \, dr \, dz = K_d A(1-\varepsilon)\int_0^H C_s I^a \, dz \quad (13)$$

where $K_d = k_i k_d S_p/v_p$ and $A = \pi R^2$. It is to be noted that K_d contains parameters pertaining to the primary catalyst particles, and therefore, K_d is independent of whether the particles are immobilized or suspended.

There are two likely loss mechanisms within the films due to the increase of catalyst layer thickness that will restrict the presence of charge carriers at the interface. One is attenuation of light due to absorption by the catalyst, and the other is the increased probability of charge carrier recombination presumably because of the increased diffusional lengths through the grain boundaries and constrictions within the microporous film. Within the bulk of the catalyst film, the extinction of light follows the exponential principle: $I = I_0 \exp[-\alpha z]$ α was determined experimentally [4] by measuring transmitted UV light intensity at 365 nm for different catalyst layer thickness. The value of α obtained was 0.6264 μm^{-1}.

5. Effect of catalyst layer thickness on photocatalytic degradation rate

It is assumed that the concentration of pollutant within the catalyst pores decreases exponentially with the effective diffusional length and is described by the following equation: $C_s = C_b \exp[-(k_f/D_e)(H-z)]$. When light is introduced from the liquid to catalyst side (Fig. 2(a)), $I = I_0 \exp[-\alpha(H-z)]$. Integrating Eq. (13), we get

$$r_t = v\frac{dC_b}{dt} = \frac{K_d A(1-\varepsilon)}{a\alpha + k_f/D_e} I_0^a C_b \times \left\{1 - \exp\left[-\left(a\alpha + \frac{k_f}{D_e}\right)H\right]\right\} \quad (14)$$

Eq. (14) indicates that the photocatalytic rate reaches a saturation value as the catalyst layer thickness increases. This can be understood if we look at the physical problem. When the catalyst film is thin, the absorption of light will not be strong enough as wavelength of light ($\lambda = 0.365$ μm) is of the same order of the magnitude as that of the film thickness, and consequently, the catalyst layer will not be active to its highest possible level. As the film thickness increases, at some point, light will be completely absorbed by the catalyst layer, and the photocatalytic reaction rate will be at maximum. With further increase in the film thickness, the rate would remain constant, as the diffusional length of the charge carrier to the catalyst–liquid interface will not change. In order to facilitate the analysis of the effect of internal mass transfer factor on the photocatalytic reaction rate, an ideal maximum reaction rate is defined at which the internal mass transfer resistance factor, k_f, is zero and catalyst layer thickness, H, is infinite. Accordingly, the maximum reaction rate is given by $r_{max} = [K_d A(1-\varepsilon)/a\alpha] I_0{}^a C_b$. Therefore,

$$\frac{r_t}{r_{max}} = \left[\frac{1}{1 + k_f/(a\alpha D_e)}\right] \times \left[1 - \exp\left\{-\left(a\alpha + \frac{k_f}{D_e}\right)H\right\}\right] \quad (15)$$

Fig. 6 shows the effect of internal mass transfer resistance factor on the degradation rate for different catalyst layer thickness. Obviously, with the increase of k_f, the reaction rate decreases significantly, particularly when the catalyst film is thick.

When the light is introduced from the catalyst side (Fig. 2(b)), integration of Eq. (13) gives

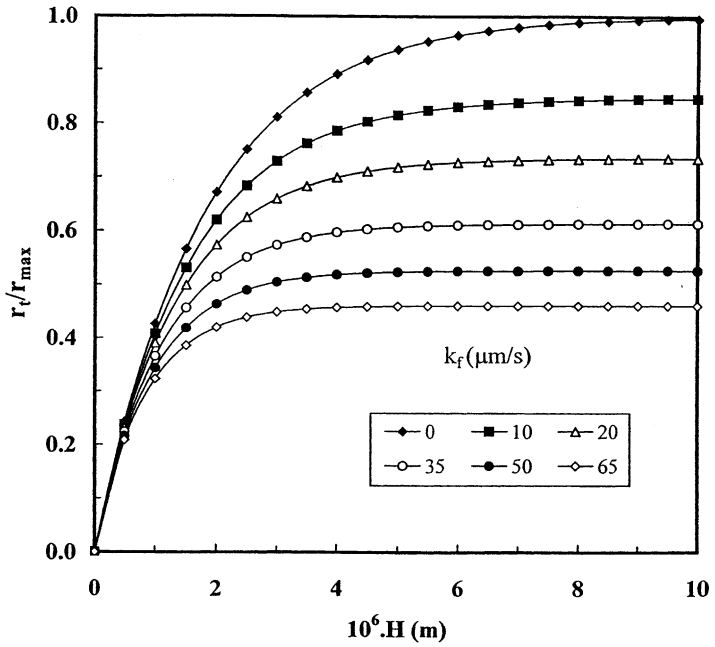

Fig. 6. Influence of internal mass transfer on phototcatalytic degradation rate for LC illumination ($a = 0.89$, $\alpha = 6.3 \times 10^5\ \mathrm{m}^{-1}$ and $D_e = 1.0 \times 10^{-10}$).

$$r_t = v\frac{dC_b}{dt} = \frac{K_d A(1-\varepsilon)}{(k_f/D_e) - a\alpha} I_0^a C_b \times \left[\exp(-a\alpha H) - \exp\left(-H\frac{k_f}{D_e}\right)\right] \quad (16)$$

Contrary to Eq. (14), Eq. (16) indicates that there exists an optimum catalyst layer thickness at which the degradation rate is at maximum. The optimum thickness is obtained by equating $dr_t/dH = 0$ and is given by $H_{opt} = \ln[a\alpha D_e/k_f]/[a\alpha - k_f/D_e]$. When the film is thin, the absorption of the light is not strong enough, and consequently, the catalyst layers in contact with the liquid is not be active to its highest possible level. As the film thickness increases, at some point the penetration depth of light will be such that most of the electrons and holes are generated relatively close to the solid–iquid interface. The photocatalytic reaction rate will be about maximum at this point. With further increase in the film thickness (thicker film), the charge carriers generated relatively far from the liquid–catalyst interface, and consequently, are more susceptible to recombination loss. For SC illumination, a further increase of film thickness will lower the photocatalytic reaction rate. This is in contrast to LC illumination, where the rate remains constant. For SC illumination, the expression of r_{max} (similar to LC illumination case) can be obtained and the dimensionless rate is given by:

$$\frac{r_t}{r_{max}} = \left[\frac{1}{\{k_f/(a\alpha D_e) - 1\}}\right] \times \left[\exp(-a\alpha H) - \exp\left\{-\left(\frac{k_f}{D_e}\right)H\right\}\right] \quad (17)$$

The expected behavior based on the model of the effect of k_f value on the photocatalytic degradation rate is shown in Fig. 7. Similar to case 1 (LC illumination), k_f has a negative effect on the reaction rate. However, in the present case there exists an optimum catalyst layer thickness, and the optimum catalyst layer thickness decreases with the increase of k_f. In reality, it is impossible to obtain the maximum reaction rate as defined above because for a given catalyst layer thickness, k_f is never zero. Therefore, a new $r_{max,p}$ was

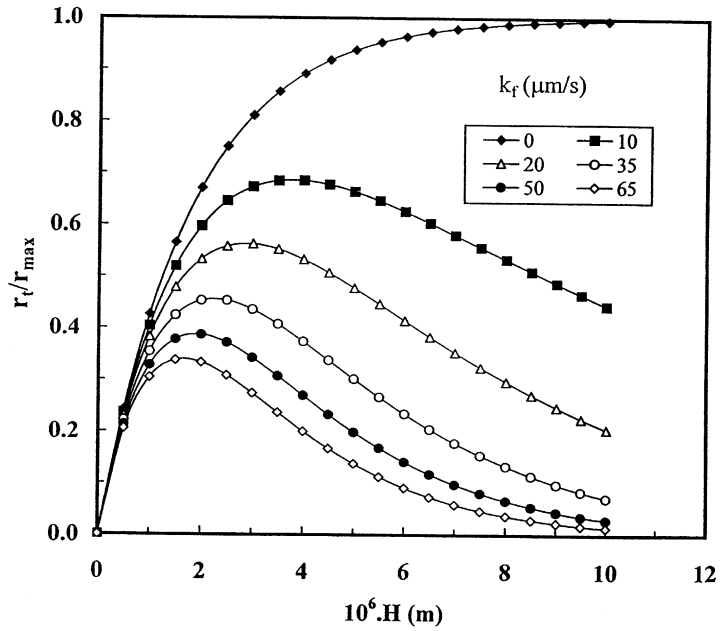

Fig. 7. Influence of internal mass transfer on photocatalytic degradation rate for SC illumination ($a = 0.89$, $\alpha = 6.3 \times 10^5\,\mathrm{m}^{-1}$ and $D_e = 1.0 \times 10^{-10}$).

defined for LC illumination by letting $H \to \infty$ and $k_f \neq 0$. From Eq. (14) we get

$$r_{max,p} = \left[\frac{K_d A(1-\varepsilon)}{(a\alpha + k_f/D_e)}\right] I_0^a C_b \quad \text{(LC illumination)} \tag{18}$$

For SC illumination, we get

$$r_{max,p} = \frac{K_d A(1-\varepsilon)}{k_f/D_e - a\alpha} I_0^a C_b \left\{\left(\frac{k_f}{a\alpha D_e}\right)^{(a\alpha D_e/a\alpha D_e - k_f)} - \left(\frac{k_f}{a\alpha D_e}\right)^{(k_f/a\alpha D_e - k_f)}\right\} \quad \text{(SC illumination)} \tag{19}$$

and accordingly we have

$$\frac{r_t}{r_{max,p}} = 1 - \exp\left[-\left(a\alpha + \frac{k_f}{D_e}\right) H\right] \quad \text{(LC illumination)} \tag{20}$$

$$\frac{r_t}{r_{max,p}} = \frac{\exp(-a\alpha H) - \exp(-Hk_f/D_e)}{(k_f/a\alpha D_e)^{(a\alpha D_e/a\alpha D_e - k_f)} - (k_f/a\alpha D_e)^{(k_f/a\alpha D_e - k_f)}} \quad \text{(SC illumination)} \tag{21}$$

Experiments were performed for photocatalytic degradation of benzoic acid using different catalyst layer thickness for both SC and LC illumination configuration. Experimental results as well as calculated values of $(r_t/r_{max,p})$ for different k_f values from Eqs. (20) and (21) are shown in Figs. 8 and 9 respectively. Experimental results do indeed show that photocatalytic rate goes through a maximum for SC illumination while it is constant for LC illumination when catalyst film is thick. The best k_f values obtained when the experimental data were fitted (using Marquardt method of least-square approximation technique) to the above equations are respectively $1.48 \times 10^{-5}\,\mathrm{m/s}$ (LC illumination) and $1.65 \times 10^{-5}\,\mathrm{m/s}$ (SC illumination). The literature reported value of k_{rxn} for benzoic acid is $1.445 \times 10^{-4}\,\mathrm{m/s}$ [10] and therefore, is one order of magnitude higher

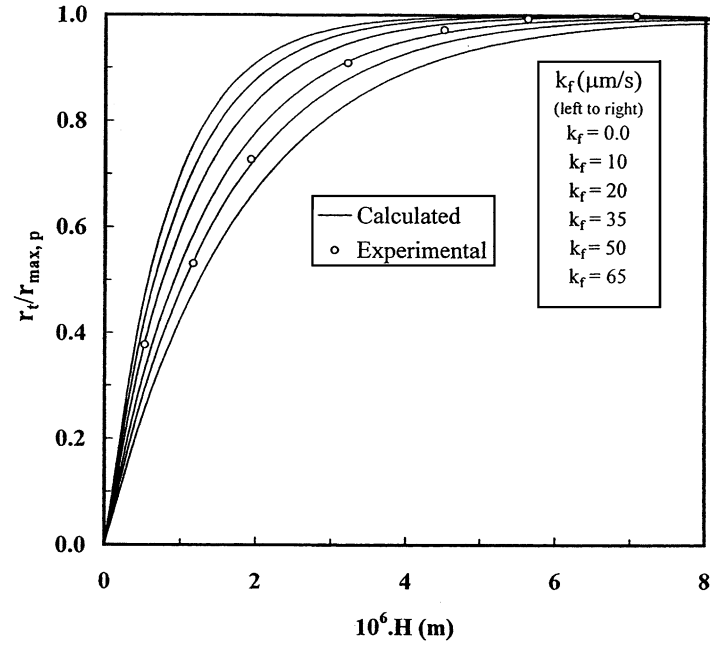

Fig. 8. Experimental determination of k_f for LC illumination ($a = 0.89$, $\alpha = 6.3 \times 10^5\,m^{-1}$, $D_e = 1.0 \times 10^{-10}\,m^2/s$, $A = 0.002\,m^2$, $T = 303\,K$, $v = 1.45 \times 10^{-4}\,m^3$ and $Re = 427$).

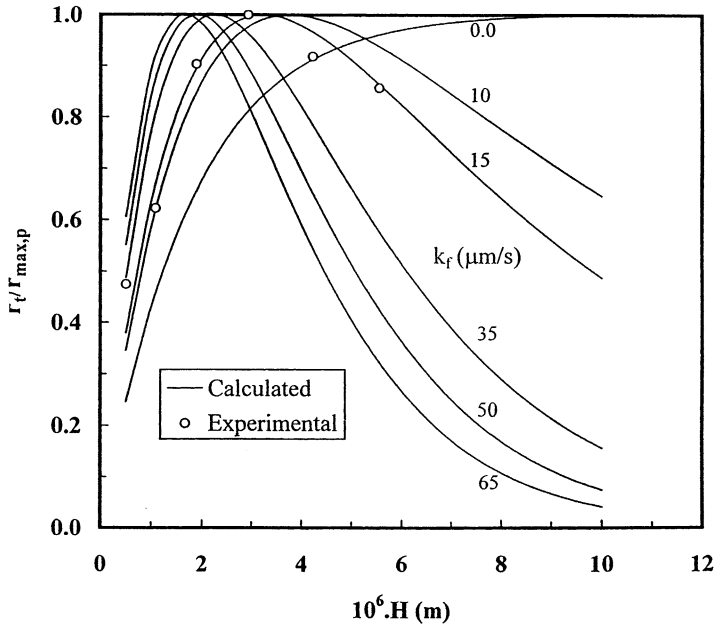

Fig. 9. Experimental determination of k_f for SC illumination ($a = 0.89$, $\alpha = 6.3 \times 10^5\,m^{-1}$, $D_e = 1.0 \times 10^{-10}\,m^2/s$, $A = 0.002\,m^2$, $T = 303\,K$, $v = 1.45 \times 10^{-4}\,m^3$ and $Re = 427$).

than k_f values obtained above. It is to be noted that the overall rate depends on all three rates described in Eq. (1). However, $k_{m,ext}$ can be reduced to significantly lower values by increasing mixing (or flow rate), and k_{rxn} can be increased somewhat by increasing light intensity. The internal mass transfer resistance is difficult to alter as it depends on catalyst layer thickness and one must use thickness at least close to the optimal value otherwise overall rate will also decrease.

6. Conclusions

In this work, effect of mass transfer and catalyst layer thickness on photocatalytic degradation of benzoic acid over Degussa P25 TiO_2 thin film supported on Pyrex glass substrate was investigated. A rational approach was proposed for the determination of external and internal mass transport parameters. Experimental results indicate that the overall rate at times is controlled by internal mass transfer resistance, which is difficult to alter. Several model parameters, namely, external mass transfer coefficient, dynamic adsorption equilibrium constant, adsorption rate constant, internal mass transfer coefficient, and effective diffusivity were determined experimentally using benzoic acid as a model component. Experiments were also conducted to determine the effect of catalyst layer thickness on photocatalytic degradation rate for both SC and LC illumination configurations. It was observed that there exists an optimum catalyst layer thickness for SC illumination while the rate reaches a saturation value for LC illumination. Ideal thickness found out from this study was around 5 μm.

Acknowledgements

The authors like to acknowledge the financial support provided by the National University of Singapore.

References

[1] A.K. Ray, A.A.C.M. Beenackers, AIChE J. 43 (1997) 2571.
[2] D.W. Chen, A.K. Ray, Water Res. 32 (1998) 3223.
[3] P.S. Mukherjee, A.K. Ray, Chem. Eng. Technol. 22 (1999) 253.
[4] A.K. Ray, Chem. Eng. Sci. 54 (1999) 3113.
[5] A.K. Ray, A.A.C.M. Beenackers, European Patent, 96200942.9-2104 (1996).
[6] A.K. Ray, A.A.C.M. Beenackers, AIChE J. 44 (1998) 477.
[7] A.K. Ray, A.A.C.M. Beenackers, Catal. Today 40 (1998) 73.
[8] K. Vinodgopal, S. Hotchandani, P.V. Kamat, J. Phys. Chem. 97 (1993) 9040.
[9] U. Periyathamby, A.K. Ray, Chem. Eng. Technol. 22 (1999) 881.
[10] D.W. Chen, M. Sivakumar, A.K. Ray, Dev. Chem. Eng. Miner. Process. 8 (2000) 505.
[11] D.W. Chen, A.K. Ray, Appl. Catal. B 23 (1999) 143.